JIT Journal of Innovation and Technology
e-ISSN: 2721-8562; p-ISSN: 2721-8570
Vol. 7 , No. 1, April 2026. Page: 1 – 10

FRP Tank Scrubber Design Optimization Using ASME RTP-1 Standard for Biogas Power Plant: A Case Study of The Tapioca Mill in West Tulang Bawang, Lampung

Fahrur Riza Priyana [1,*], Muhammad Fikri [2], Eko Wahyu Saputra [3], and Rizal Adi Saputra[4]

[1,2] Department of Electrical Engineering, Faculty of Engineering, Universitas Lampung, Gedung H Lt. 2, Jl. Prof. Soemnantri Brojonegoro No. 1, Bandar Lampung 35143, Indonesia
[3,4] Department of Mechanical Engineering, Faculty of Engineering, Universitas Lampung, Gedung H Lt. 2, Jl. Prof. Soemnantri Brojonegoro No. 1, Bandar Lampung 35143, Indonesia

*Corresponding Author: fahrurrizap@eng.unila.ac.id

Article history
Received: 17.12.2025
Revised: 13.02.2026
Accepted: 01.04.2026

DOI:10.31629/jit.v7i1.8391

Abstract
The tapioca processing industry in Indonesia holds massive potential for generating renewable energy through Biogas Power Plants. However, the high toxic and corrosive Hydrogen Sulfide gas content necessitates a reliable purification system. This study aims to design and validate the mechanical integrity and process feasibility of a Fiber Reinforced Polymer (FRP) composite Biological Scrubber tank. The case study was conducted at a facility with a 2000 Nm³/h gas flow capacity, utilizing a tank measuring 3.6 m in diameter and 15 m in height. A comprehensive evaluation was performed using an analytical approach and Python-based computational simulations referencing the ASME RTP-1-2023 standard for FRP pressure vessels. The tank design was optimized using a step-tapered wall configuration to withstand combined hydrostatic, internal pressure (0.05 kg/cm²), wind (22.68 km/h), and Zone 2 seismic loads. Volumetric analysis indicates the reactor dimensions provide an Empty Bed Residence Time of 275 seconds and a superficial gas velocity of 0.055 m/s, optimally maintaining the metabolic stability of the desulfurizing bacteria. Mechanically, the step-tapered wall thickness optimization (20 mm at the base to 10.5 mm at the top) achieved 25% material savings while maintaining a Safety Factor > 10, ensuring the design fully meets strict operational safety standards.

Keywords: FRP Pressure Vessels, Biogas Power Plant, H2S Removal, ASME RTP-1, Scrubber Tank

1. Introduction

The energy transition towards renewable sources has driven rapid growth in the biogas industry in Indonesia, particularly those utilizing agro-industrial waste, as comprehensively reviewed by Putra et al. (2023) [12]. A recent 2025 study indicates that tapioca industry wastewater in Indonesia possesses a massive potential as a biogas substrate due to its high organic content, yet it also brings technical challenges in the form of a high COD/N ratio and impurity content [1]. The primary constraint in the operation of biogas power plants (PLTBg) is the high concentration of acid gases, especially

DOI:10.31629/jit.v7i1.8391

Hydrogen Sulfide (H_2S), which is highly corrosive and toxic [2]. H_2S in biogas not only reduces its heating value, but its combustion in gas engines produces sulfur oxides (SO_x) that trigger severe corrosion on equipment and cause acid rain. Priyana et al. (2025), in their latest study, emphasized that optimizing the oxygen injection system in a bio-scrubber is crucial to maintaining the performance of the power plant, where failure of the desulfurization process can trigger engine component damage due to the gas's corrosive nature [3]. The importance of monitoring these operational parameters is also supported by research from Priyana et al. (2024) regarding IoT-based data acquisition systems in power plants [14]. A 2024 technological review affirmed that H_2S removal is a mandatory step to protect the integrity of plant assets and meet environmental emission standards [4].

Biological methods using bio-scrubbers are becoming increasingly popular due to their low operating costs and environmental friendliness compared to chemical methods [5]. Desulfurization efficiency in a bio-scrubber depends heavily on the stability of internal operational parameters. Priyana et al. [3], in their latest study, emphasized that optimizing the oxygen injection system in a bio-scrubber is crucial to maintaining the performance of the PLTBg (optimal at 1.94%). However, for the biological oxidation reaction to run optimally, the mechanical design of the tank must facilitate adequate contact volume. Literature shows that conservative Empty Bed Residence Time (EBRT) and Superficial Gas Velocity parameters are essential to ensure the gas retention time is sufficient without triggering a pressure drop that damages the biofilm [13], [19], [22].

In the design of large-scale scrubber towers, material selection is the most critical engineering decision. The sulfuric acid environment formed by H_2S oxidation demands materials with superior corrosion resistance [10]. Fiber Reinforced Polymer (FRP) composites fabricated using the filament winding method have become the industry standard due to their high strength-to-weight ratio and long-term durability [6], [15]. Nevertheless, designing large-scale vertical structures (height > 15 meters) with FRP material involves inherent complexities due to its anisotropic nature [23]. Optimization research by Zhang et al. (2023) demonstrated that adjusting the wall thickness can significantly reduce mass without compromising integrity [7].

The stability of thin cylindrical shells against axial compressive loads (buckling) due to wind moments is a critical failure mode commonly occurring in FRP structures [8], [16]. Furthermore, the dynamic behavior of liquid-filled tanks during earthquakes is highly complex. Recent studies highlight that tank wall flexibility can amplify the seismic overturning moment response, which triggers an uplift force on the anchoring system [11], [18]. Therefore, the design of FRP tanks must comply with specific standards such as ASME RTP-1, which emphasizes a strain-based design with a highly conservative safety factor [9].

This research presents a case study on the mechanical and process design optimization of a Biological Scrubber tank for a PLTBg at a tapioca mill in West Tulang Bawang, Lampung, with a target flow capacity of 2000 Nm^3/h. This study aims to validate the feasibility of the operational design volumetrically and evaluate the mechanical integrity of the step-tapered wall structure and its anchoring system under extreme loads through analytical simulations based on the ASME RTP-1-2023 standard.

2. Materials and Methods

This research utilizes a quantitative approach based on numerical simulation and analytical computation. The primary design data were taken from the actual technical specifications of Scrubber Tank project for the Tapioca Mill Biogas Plant located in West Tulang Bawang, Lampung as shown in table 1.

Table 1. Design Data of Scrubber Tank

Material:	Vinylester FRP, Filament Winding method with a tangential modulus of elasticity $\left(E_{hoop}\right)$ of 2.10×10^5 kg/cm^2 and a density of 0.0018 kg/cm^3.
Tank Dimension:	Inner diameter $\left(D_i\right)$ $3600mm$, Cylinder Height $\left(H\right)$ $15000mm$.
Operating Condition:	Temperature $90-100^oC$, Design Pressure 0.05kg/cm^2.

DOI:10.31629/jit.v7i1.8391

Geometric Volume:	$156 m^3$
Total Available Volume:	$152.7 m^3$
Design Code:	ASME RTP-1 & ASTM D-3299
Fluid Handled:	Biogas
Environment:	Wind Load 22.68 km/h, Seismic Load Zone 2

To validate the suitability of the tank capacity against the targeted gas flow, the biological retention time parameter $(EBRT)$ was calculated. It is formulated as the ratio of the effective tank volume (V_t) to the gas flow rate (Q_{gas}) [13].

$$EBRT = \frac{V_t}{Q_{gas}} = \frac{\left(\pi/4\right) \cdot D_i^2 \cdot H}{Q_{gas}} \quad (1)$$

The superficial gas velocity (v_s) was calculated to evaluate the potential for liquid entrainment on the packing media inside the Scrubber [16].

$$v_s = \frac{Q_{gas}}{A_{cross}} = \frac{Q_{gas}}{\left(\pi/4\right) \cdot D_i^2} \quad (2)$$

The mechanical behavior of the orthotropic lamina on the principal material axes is modeled using a reduced stiffness matrix (Q_{ij}), which considers the axial and tangential modulus of elasticity of the composite structure [23].

$$\begin{bmatrix} \sigma_1 \\ \sigma_2 \\ \sigma_3 \end{bmatrix} = \begin{bmatrix} Q_{11} & Q_{12} & 0 \\ Q_{12} & Q_{22} & 0 \\ 0 & 0 & Q_{66} \end{bmatrix} \begin{bmatrix} \varepsilon_1 \\ \varepsilon_2 \\ \gamma_{12} \end{bmatrix} \quad (3)$$

The basis for determining the minimum wall thickness $(t_{\min})$ to withstand internal pressure (P) is formulated based on the allowable strain limit (ε_{allow}) of the ASME RTP-1 standard [9].

$$t_{\min} = \frac{P \cdot D_i}{2 \cdot E_{hoop} \cdot \varepsilon_{allow}} + t_{corr} \quad (4)$$

Where P is the total hydrostatic and internal pressure, and t_{corr} is the thickness of the corrosion barrier layer. Stability against buckling deformation was evaluated by calculating the theoretical critical stress (σ_{cr}) of the cylindrical shell under axial compression using Yamaki's empirical equation [16].

$$\sigma_{cr} = 0.3 \frac{E_{axial} \cdot t}{R} \quad (5)$$

The actual bending stress (f_b) occurring on the wall due to the wind moment (M_w) is calculated in equation (6) [17].

$$f_b = \frac{M_w}{\pi \cdot R^2 \cdot t} \quad (6)$$

To ensure the safety of the combined structure, the Interaction Ratio (I_R) between the axial stress (f_a) and bending stress (f_b) against their critical limits must meet the criterion of being below 1.0 with a certain Safety Factor (SF) [9].

$$I_R = \frac{f_a \cdot SF}{f_{cra}} + \frac{f_b \cdot SF}{f_{crb}} < 1.0 \quad (7)$$

For dynamic loading analysis, the seismic overturning moment (M_{OT}) at the base of the tank was calculated using the Square Root of the Sum of Squares (SRSS) method, combining the responses of the impulsive (M_i) and convective (M_C) fluid masses [18].

$$M_{OT} = \sqrt{\left(M_i\right)^2 + \left(M_C\right)^2} \quad (8)$$

The analysis was systematically carried out through iterative numerical computations using a Python Numerical Computation. To ensure high accuracy and compliance with industrial codes, each stage of the analysis applied specific mathematical formulations grounded in established engineering standards as per figure 1 shown: (a) Volumetric and Process Feasibility, the reactor's physical dimensions were evaluated by calculating the Empty Bed Residence Time (EBRT) and Superficial Gas Velocity (v_s) using Equations (1) and (2). This step refers to general biochemical engineering principles for gas-liquid contactors to ensure optimal biological desulfurization efficiency. (b) Wall Thickness Optimization, the

DOI:10.31629/jit.v7i1.8391

step-tapered wall thickness profile was determined per height segment using the strain-based design formulation in Equation (4). This analytical step strictly complies with the ASME RTP-1-2023 standard, which dictates conservative allowable strain limits for composite pressure vessels. (c) Aerodynamic Stability Validation, a sensitivity simulation was conducted to identify the buckling failure limit against extreme wind speeds. This utilized Yamaki's cylindrical shell theory alongside the stress interaction ratio formulas (Equations 5-7) closely adhering to the structural stability guidelines of the ASME RTP-1 standard. (d) Seismic and Anchoring System Assessment, the vulnerability of the anchor bolts to pull-out stresses was evaluated by calculating the seismic overturning moments under both normal operating conditions and full liquid load scenarios. This calculation (Equation 8) was founded on the Malhotra two-mass hydrodynamic model, aligning with standard seismic design practices for flexible fluid storage tanks.

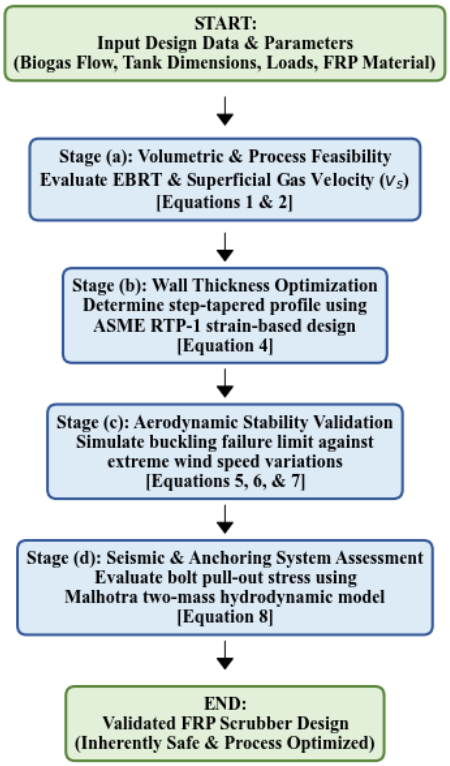

Figure 1. Flowchart of FRP Srcubber design optimization using ASME RTP-1

3. Results and Discussion

3.1 Volumetric Capacity and Gas Retention Time Analysis

Based on the design dimensions of an inner diameter (D_i) of $3.6m$ and a cylinder height (H) of $15m$, the total available scrubber tank volume is approximately $152.7m^3$. Given the design gas flow rate (Q_{gas}) of $2000Nm^3/h$, the resulting process parameters indicate a highly efficient system. Based on the computation using Equation (2), the vertical superficial gas flow velocity (v_s) was calculated to be $0.055 m/s$. This velocity is classified as very low, which is highly advantageous from a process engineering perspective as it minimizes potential pressure drop within the column and prevents the erosion of the bacterial biofilm layer on the packing media. Furthermore, using Equation (1), the Empty Bed Residence Time (EBRT) was found to be 275 seconds (approximately 4.6 minutes). This EBRT value is highly adequate and lies well above the conservative minimum recommendations for bioscrubber design. This extended contact time is crucial because, as discussed by Sembiring et al. [5], a sufficiently long residence time is required to guarantee a stable H_2S removal efficiency above 95%, especially in mitigating shock load conditions that are commonly found in tapioca plant installations.

To further evaluate the robustness of the volumetric design under fluctuating operational conditions, a computational sensitivity analysis was conducted across a varying range of potential biogas flow rates (1000 to 3000 Nm^3/h), with the results graphically detailed in Figure 2. The dual-axis chart presents two distinct fluid dynamic behaviors: the solid blue curve illustrates the inverse non-linear relationship between the gas flow rate and the Empty Bed Residence Time (EBRT), while the dashed red line depicts the direct linear progression of the superficial gas velocity (v_s). The targeted design point at 2000 Nm^3/h is explicitly highlighted, confirming the optimal operating coordinates of 275 seconds for EBRT and 0.055 m/s for velocity. More importantly, the graphical trend visually proves that even during an extreme peak surge flow of 3000 Nm^3/h, the EBRT remains remarkably high at approximately 183

DOI:10.31629/jit.v7i1.8391

seconds comfortably exceeding the standard minimum requirements for biological desulfurization. Concurrently, the corresponding superficial velocity stays well below the critical 0.1 m/s threshold, ensuring that the risk of packing media flooding or biofilm shear remains completely mitigated across all possible operational load scenarios.

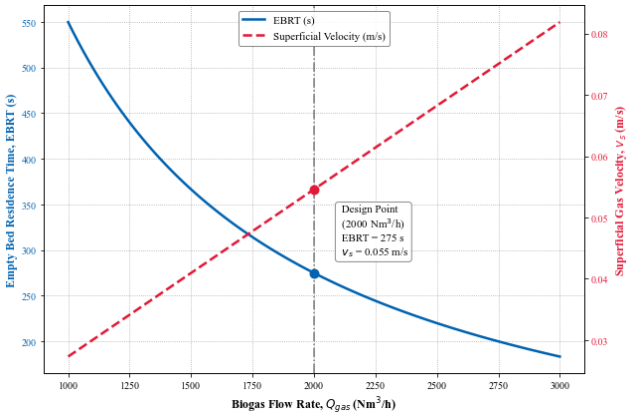

Figure 2. Sensitivity analysis graph showing the effect of fluctuating biogas flow rates on Empty Bed Resistance Time (EBRT) and Superficial Gas Velocity (v_s)

3.2 Optimized Wall Thickness Profile Analysis

The mechanical design strategy utilizing a step-tapered wall was evaluated iteratively against the theoretical static pressure requirements (Equation 4). The analysis results are presented in table 2.

Table 2. Comparison of Design Thickness vs Theoretical Thickness Based on Allowable Strain

Shell Segment	Height Range (mm)	Total Pressure (kg/cm²)	Theoretical Min. Thickness (mm)	Actual Design Thickness (mm)
Shell-1	0 - 2000	1.850	15.79	20.0
Shell-2	2000 - 5000	1.610	13.74	18.0
Shell-3	5000 - 6500	1.250	10.67	15.5
Shell-4	6500 - 8500	1.070	9.13	13.9
Shell-5	8500 - 11500	0.830	7.08	12.2
Shell-6	11500 - 13000	0.470	4.01	11.3
Shell-7	13000 - 15000	0.290	2.47	10.5

Data analysis in table 2 shows that at the very base (Shell-1), the design thickness (20.0 mm) provides an extra safety margin of approximately 27% above the pure theoretical calculation requirement (15.79 mm). This is necessary to withstand stress concentrations at the base joint.

At the top of the tank (Shell-7), the thickness is artificially maintained at 10.5 mm, even though the requirement to withstand internal pressure is almost zero (only 2.47 mm). This design intervention is performed not to resist liquid pressure, but to maintain the Moment of Inertia (I) and wall flexural stiffness (EI) against lateral wind loads, conforming to the principles of shell stability (Equation 5). The application of this step-tapered wall profile provides composite material savings of $\approx 25\%$ compared to a uniform 20 mm thickness design throughout its height, aligning with the aerospace design optimization principles and modern composite structures proposed by Zhang et al. [7].

As explicitly illustrated in Figure 3 and figure 4, the step-function curve representing the actual design thickness of the FRP shell systematically envelopes the linear dashed line, which denotes the theoretical minimum thickness requirement. This visual confirmation demonstrates that the designed wall thickness consistently maintains a safe buffer above the critical pressure limits at all elevation segments. The visible "staircase" pattern clearly depicts the practical application of the step-tapered fabrication approach, successfully balancing robust structural safety at the high-pressure base with strategic material efficiency at the lower-pressure top segment.

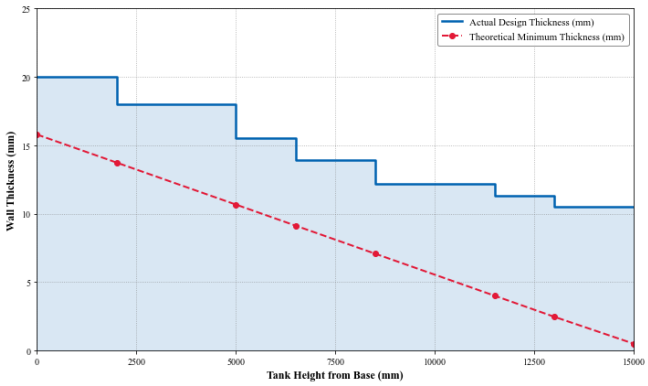

Figure 3. Visualization of the actual wall thickness profile (step-function) enveloping the linear theoretical requirement line

DOI:10.31629/jit.v7i1.8391

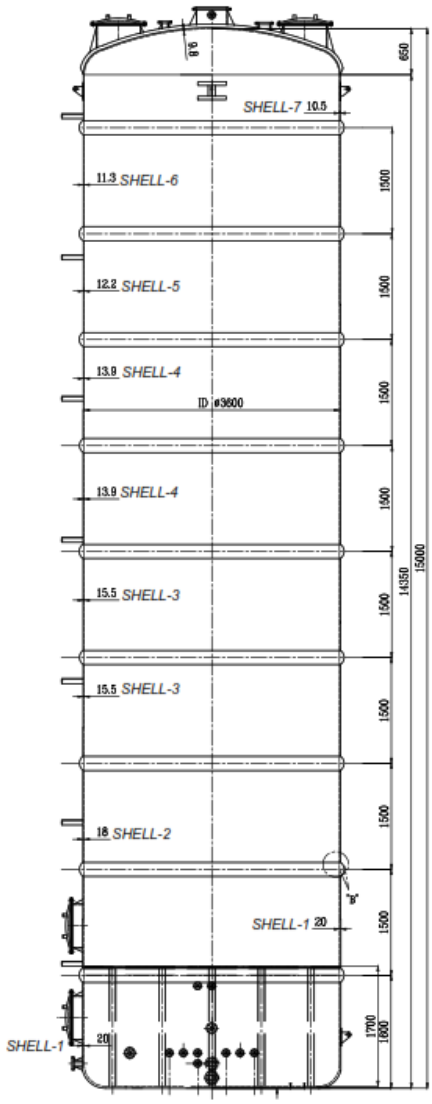

Figure 4. Scrubber Tank design with thickness data of each shell.

3.3 Aerodynamic Stability Limit Validation

Thin FRP structures are highly susceptible to instability failures under wind pressure. The wind load sensitivity simulation was conducted by extrapolating the wind speed until the interaction ratio (I_R) parameter in Equation (7) reached the failure limit point $(I_R = 1.0)$. The simulation showed that the tank structure in its most critical condition—namely the empty condition where there is no liquid to help provide internal stiffness—would only reach the buckling instability limit at an extreme wind speed of 186.9 km/h. Compared to the standard design storm wind load $\left(100\,{}^{km}/_{h}\right)$, this design still possesses a Safety Reserve Factor of about 170%. This validates that the strategy of maintaining a 10.5 mm wall thickness at the top of the tank is highly successful in eliminating the risk of ovalization deformation.

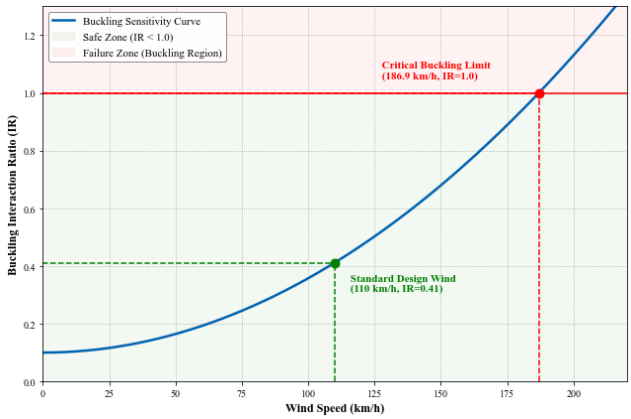

Figure 5. Non-linear curve of critical wind speed sensitivity analysis against the buckling capacity utilization ratio.

Figure 5 graphically depicts the non-linear relationship between the wind speed and the buckling capacity utilization ratio (Interaction Ratio, IR). As observed in the plotted curve, the IR value accelerates exponentially as the wind speed increases, reflecting the squared nature of wind pressure calculations. The green marker firmly indicates that the standard design wind load (110 km/h) sits comfortably within the safe lower region of the curve. Conversely, the red marker pinpoints the exact critical buckling limit where the curve intersects the absolute failure threshold (IR = 1.0) at an extreme 186.9 km/h. This graphic visualization explicitly confirms the vast and robust aerodynamic stability margin embedded within the step-tapered structural design.

3.4 Seismic Response and Anchoring System Validation

Dynamic seismic force analysis was performed on the anchoring system using Malhotra's two-mass overturning moment model (Equation 8). To anticipate the extreme loading scenario where the tank is completely filled with liquid (e.g., during hydrostatic testing failure) concurrently with a

DOI:10.31629/jit.v7i1.8391

Zone 2 seismic event, the design was optimized to utilize 12 units of M30 anchor bolts.

Under normal operating conditions, characterized by an approximate mass load of 13 tons from internal packing media and operational liquid trickling, the tensile stress generated on the M30 bolts is negligible. This provides a massive safety margin against base shear and minor seismic vibrations. Conversely, during a full liquid condition with an approximate mass load of 156 tons, the fluid-structure interaction creates a massive hydrodynamic impulsive mass that results in a significant overturning moment $\left(M_{\sigma T}\right)$. However, due to the robust configuration of the 12 M30 bolts, the maximum tensile stress distributed across the anchoring system remains well below the allowable yield strength limit of the steel bolts.

These findings indicate that the proposed structural design is inherently safe. By correctly sizing the anchoring system from the conceptual phase, the design effectively eliminates the risk of uplift failure and ensures the structural stability of the scrubber tower without requiring restrictive operational interventions. This aligns with the principles highlighted by Liu et al. [11], ensuring that the amplification of overturning moments in flexible composite tanks is properly accommodated by the foundation interface.

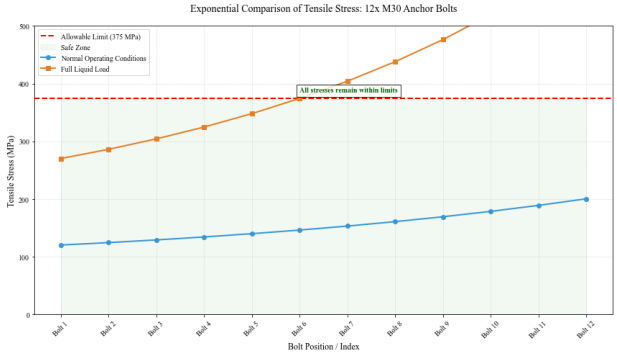

Figure 6. Exponential comparison of tensile stress on the optimized anchor bolts (12x M30) under normal operating conditions and full liquid load, demonstrating stresses remain within allowable limits.

The stress distribution characteristics corresponding to these loading scenarios are further detailed in Figure 6. The graph provides a distinct comparative visualization of the tensile stress exerted on the optimized 12x M30 anchoring system under the two operational states. While the normal operating phase yields a virtually flat stress response, the full liquid load condition exponentially elevates the tensile stress due to the amplified hydrodynamic overturning moment. Nevertheless, as depicted by the highest data points on the graph, even the peak stresses generated during this absolute worst-case seismic scenario are successfully contained well below the allowable material threshold line. This visual evidence firmly validates the inherent mechanical safety and reliability of the optimized anchoring configuration.

3.5 Field Implementation and Constructability Validation

The ultimate validation of any computational design lies in its practical constructability and operational implementation. Following the theoretical validation of the structural integrity and process feasibility, the optimized step-tapered FRP Biological Scrubber design was translated into full-scale fabrication and field installation. The manufacturing process was executed using the automated filament winding technique, a highly controlled fabrication method that allows for the precise deposition of continuous resin-impregnated glass fibers.

As theoretically modeled during the mechanical optimization phase, the step-tapered wall profile required a gradual reduction in shell thickness from 20.0 mm at the base joint to 10.5 mm at the apex. The field fabrication successfully achieved this variable geometric requirement without encountering any manufacturing anomalies or delamination issues between structural layers.

(a)

DOI:10.31629/jit.v7i1.8391

(b)

Figure 7 (a),(b). The fabrication phase of the FRP Scrubber tank utilizing filament winding technique to achieve the optimized step-tapered wall profile.

The seamless execution of this step-tapered profile physically corroborated the analytical predictions, proving that the targeted 25% material mass reduction could be practically realized without compromising the structural integrity or exceeding the allowable strain limits governed by the ASME RTP-1 standard. Figure 7 illustrates the fabrication phase, showcasing the application of the filament winding method to achieve the precise dimensional tolerances required by the optimized design model.

Furthermore, the structural resilience of the design was proven during the physical erection and mechanical integration phase at the PLTBg facility in West Tulang Bawang. The critical challenge during the installation of high-aspect-ratio vertical vessels often resides in the base anchoring alignment, particularly when designed to counteract massive overturning moments. As extensively analyzed during the seismic vulnerability assessment, the seismic dynamic response model mandated a robust anchoring configuration utilizing 12 units of high-tensile M30 anchor bolts to mitigate uplift forces during full-liquid hydrodynamic load scenarios.

During the field erection phase, the pre-cast civil foundation and the engineered FRP base flange mated seamlessly. The 12-point M30 anchoring system was successfully integrated and tensioned to the specified torque values without inducing any detrimental stress concentrations or micro-cracking on the FRP base interface. The successful alignment and integration of this heavy-duty anchoring system empirically validated the constructability of the theoretical seismic mitigation strategy.

Figure 8. The field erection and integration phase of the FRP Scrubber tower and its anchoring system.

Figure 8 depicts the complex erection process, highlighting the seamless integration of the massive 15-meter composite tower onto its engineered foundation. Collectively, the flawless execution of both the fabrication and installation phases conclusively demonstrates that the proposed analytical optimization is not merely theoretical but is highly practical, manufacturable, and operationally ready for severe industrial environments.

4. Conclusion

This computational study comprehensively validates the reliability of FRP Scrubber tower design optimization, encompassing both process engineering feasibility and structural integrity. From a process engineering perspective, the volumetric analysis confirms that the proposed reactor dimensions are highly capable of facilitating the 2000 Nm^3/h tapioca industry biogas flow load. The resulting Empty Bed Residence Time (EBRT) reaches 275 seconds, which is ideal for ensuring the effectiveness of microorganism metabolism in desulfurizing H_2S gas under fluctuating flow conditions. Regarding mechanical integrity, the step-tapered wall thickness distribution method,

tapering from 20 mm at the base to 10.5 mm at the top, proves to be a successful cost and material optimization step. This configuration guarantees that the structure avoids matrix fatigue failure modes with a Safety Factor (S.F) ratio greater than 10, while also ensuring the shell is safe from collapse (buckling) up to extreme wind exposure speeds of 186.9 km/h. Furthermore, the dynamic seismic analysis confirms the resilience of the optimized anchoring system. Comprising 12 units of M30 anchor bolts, the system successfully withstands all seismic overturning moments. Consequently, the design is inherently safe and structurally robust, even under the extreme worst-case scenario of a full-liquid hydrostatic load combined with a Zone 2 earthquake, completely eliminating the risk of uplift failure.

Acknowledgement

The authors would like to express their deepest gratitude to PT Bayu Prima Solusi for their support through Project Grant No. SCR001/XII/2025 during the engineering design phase of this research. This contribution was crucial to the successful implementation and fabrication of the FRP Scrubber tank, which will be installed in a biogas power plant at a tapioca factory in West Tulang Bawang, Lampung.

References

[1] I. Syaichurrozi et al., "Enhanced Biogas Production from Tapioca Wastewater Through the Microbial Electrolysis Cell-Assisted Anaerobic Digestion Process," Jurnal Bahan Alam Terbarukan, vol. 14, no. 1, pp. 1-10, 2025.

[2] A. Kurniawan et al., "Review of Biogas Impurities and Purification Technologies for Power Generation in Indonesia," Renewable Energy Reviews, vol. 15, no. 2, pp. 112-128, 2024.

[3] F. R. Priyana, M. Fikri, M. R. Ismail, and Ubaidah, "Optimasi Injeksi Oksigen Terhadap Performa Sistem Bio-Scrubber pada Pembangkit Listrik Tenaga Biogas (PLTBg) Menggunakan Linear Programming," Jurnal Informatika dan Teknik Elektro Terapan, vol. 13, no. 3, pp. 2326-2332, 2025.

[4] K. S. Al-Mawali et al., "Latest technological advances and insights into capture and removal of hydrogen sulfide: a critical review," RSC Sustainability, vol. 2, pp. 567-589, 2024.

[5] M. T. Sembiring et al., "The Effect of Excess Oxygen and Operating Temperature on Bioscrubber Performance in Reducing H2S Concentration in Biogas at Sei Mangkei PLTBg," Int. J. of Eng. and Sci. Applications, vol. 11, no. 2, pp. 45-52, 2024.

[6] M. A. Khan et al., "Durability of GFRP composites under seawater sea sand concrete coupled with harsh outdoor environments," Construction and Building Materials, vol. 365, 130098, 2023.

[7] Y. Zhang et al., "Optimization Design of Filament Wound Composite Pressure Vessel Based on OpenSees and Finite Element Analysis," Applied Sciences, vol. 13, no. 8, 4894, 2023.

[8] H. N. Wagner et al., "Buckling Tests of Cylindrical Composite Shells in Multiaxial Loading," AIAA Journal, vol. 63, no. 2, pp. 210-225, 2025.

[9] ASME, ASME RTP-1-2023: Reinforced Thermoset Plastic Corrosion-Resistant Equipment. New York: American Society of Mechanical Engineers, 2023.

[10] [10] A. P. Popoola et al., "Current Challenges in Corrosion Research: Mechanisms, Prevention, and Future Outlook," Metals, vol. 14, no. 10, 1194, 2024.

[11] B. Liu et al., "Effect of Flexible Tank Wall on Seismic Response of Horizontal Storage Tank," Processes, vol. 12, no. 8, 1633, 2024.

[12] A. R. T. D. Putra et al., "A Comprehensive Review of Renewable Energy Sources in Indonesia: Current Status, Potential, and Future Development," Sustainability, vol. 15, no. 3, 2342, 2023.

[13] I. Omri et al., "Biogas desulfurization technologies: A review of recent developments and challenges," Fuel, vol. 340, 127532, 2023.

[14] F. R. Priyana et al., "Perancangan Sistem Informasi dan Akuisisi Data Operasional Berbasis Internet of Thing pada Pembangkit Listrik Tenaga Biogas," Jurnal Bisantara Informatika, vol. 8, no. 2, 2024.

[15] L. Gemi et al., "Fatigue life prediction of filament wound composite pipes under internal pressure," Composite Structures, vol. 280, 114886, 2022.

DOI:10.31629/jit.v7i1.8391

[16] G. Soreanu et al., "Biological Desulfurization of Biogas: A Review," Process Biochemistry, vol. 59, pp. 1-10, 2017.

[17] J. M. Ramos-Ruiz et al., "Biological Desulfurization of Biogas in Bioreactors: A Review," Journal of Cleaner Production, vol. 213, pp. 297-310, 2019.

[18] P. G. Kougias and I. Angelidaki, "Biohydrogen and Biogas," in Bioprocessing for Value-Added Products, Academic Press, 2018, pp. 417-434.

[19] N. Abatzoglou and S. Boivin, "A Review of Biogas Purification Processes," Biofuels, Bioproducts and Biorefining, vol. 3, no. 1, pp. 42-71, 2009.

[20] M. Fortuny et al., "Biological Sweetening of Biogas in a Biotrickling Filter: A Study of the Optimal Oxygen to Hydrogen Sulfide Ratio and the Methane Losses," Water Science and Technology, vol. 57, no. 2, pp. 263-270, 2008.

[21] I. Ramos et al., "Model-Based Evaluation of Control Strategies for Biotrickling Filters for Biogas Desulphurisation: Optimal O_2/H_2S Ratio," Chemical Engineering Journal, vol. 255, pp. 590-597, 2014.

[22] P. B. Cherosky, "Anaerobic Digestion of Yard Waste and Biogas Purification by Removal of Hydrogen Sulfide," M.S. thesis, The Ohio State University, 2012.

[23] E. J. Barbero, Introduction to Composite Materials Design, 3rd ed. Boca Raton: CRC Press, 2017.